PHYSICAL REVIEW D **82,** 065007 (2010)

Quasiconformality and mass

Dennis D. Dietrich

CP^3*-Origins, Centre for Particle Physics Phenomenology, University of Southern Denmark, Odense, Denmark*

(Received 4 May 2010; published 8 September 2010)

We identify universal quasiconformal (walking) behavior in non-Abelian gauge field theories based on the mass-dependent all-order β function introduced in [D. D. Dietrich, Phys. Rev. D **80**, 065032 (2009)]. We find different types of walking behavior in the presence of (partially) massive species. We employ our findings to the construction of candidate theories for dynamical electroweak symmetry breaking by walking technicolor.

DOI: 10.1103/PhysRevD.82.065007 PACS numbers: 11.10.Hi, 12.38.Cy

I. INTRODUCTION

Here, we analyze further implications from the mass-dependent β function introduced in [1].

Regarding a variable number of active flavors breaks the two-loop scheme independence (''universality'') of the β function of non-Abelian gauge field theories. Considering a fixed number of species is legitimate for energy scales far above or far below their masses. From the viewpoint of renormalization theory, it is even legal to ignore the freezing out of heavy flavors, although this disregards important physical effects and leads to a poor convergence of the perturbative series. Oftentimes β functions for different integer numbers of flavors are glued together at the mass of the species that are switched on or off. Already with this procedure the β-function coefficients are no longer scheme independent in the above sense. The passage between different numbers of active flavors should happen gradually. Hence, we based the β function in [1] on a background field momentum subtraction scheme [2], which next to the decoupling theorem [3] also respects the Slavnov-Taylor identities [4–9]. An alternative would have been the physical charge approach [10], which, however, coincides to lowest order and is otherwise qualitatively and also quantitatively close to the background field momentum subtraction scheme (see especially Fig. 2 in [10]), where the expressions are known analytically. It turns out that threshold effects are felt more then 2 orders of magnitude away from the mass of the fermion. In [1], we combined this input with the all-order β function without threshold effects that had been conjectured in [11]. It was motivated by the $\mathcal{N} = 1$ supersymmetric Novikov-Shifman-Vainshtein-Zakharov β function, has the correct limits in exactly known cases (super Yang-Mills theory [12] or planar equivalence in a large-N_c limit [13]), and at two-loop order it reproduces the universal β function. Far away from all thresholds our β function reduces to the massless all-order β function with a fixed number of flavors, while at two-loop order it coincides with the β function in the background field momentum subtraction scheme [2].

The mass dependence of the β function is important in the context of the conformal window of non-Abelian gauge field theories. It arises from the interplay of the matter content of a theory and chiral symmetry breaking (see Fig. 1): With no or little matter [like in quantum chromodynamics (QCD)] the antiscreening of the non-Abelian gauge bosons forestalls the appearance of an infrared fixed point (A). Slightly more matter admits a perturbative Caswell-Banks-Zaks [14] fixed point (B). For this fixed point to be reached it must be situated at a value of the coupling that does not trigger chiral condensation (D). [With even more matter the theory loses asymptotic freedom (F).] Otherwise the fermions receive a dynamical mass and decouple at least partially, which makes the antiscreening dominate once more (C). Where the fixed point is almost reached (E) but chiral condensation still sets in we find the quasiconformal case. In the vicinity of the

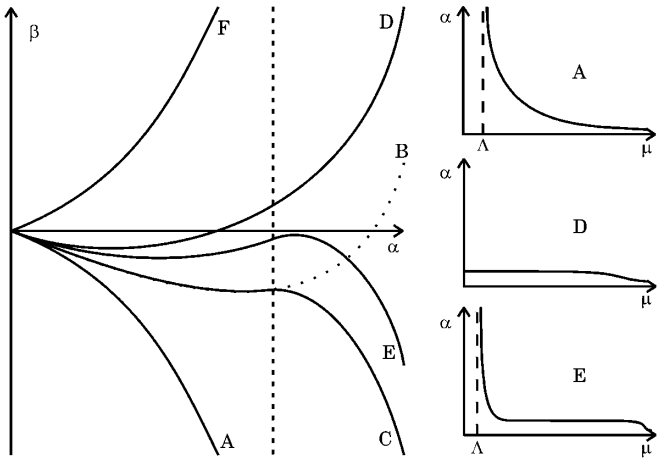

FIG. 1. Behavior of the β function as a function of the coupling $\alpha = g^2/(4\pi)$ and of the coupling as a function of the energy scale μ, depending on the matter content of the theory. (A) No or little matter; (B) existence of a perturbative Caswell-Banks-Zaks fixed point; (C) actual shape due to chiral symmetry breaking; (D) realized fixed point; (E) quasiconformal case; (F) loss of asymptotic freedom. The dashed line in the plot on the left-hand side indicates the critical values of the coupling for chiral symmetry breaking (taken from [1]).

would-be fixed point $\beta \lesssim 0$. This results in a coupling that stays almost constant (''walks'') for a large interval of energy scales at a value slightly below the critical value for chiral condensation. Once chiral condensation is finally triggered the coupling constant begins running again. What has just been said explains why taking into account the mass of the fermions is a crucial ingredient for gaining an understanding of the dynamics of the theory.

One of our motivations for conducting research into the conformal window of gauge field theories and for the study [15] is the identification of quasiconformal [16] technicolor [17] models that are consistent with presently available electroweak precision data [18,19]. These models feature a rich collider phenomenology accessible to the Large Hadron Collider (LHC) [20], dark matter candidates [21], and are interesting models for studies in the AdS/CFT framework [22]. They break the electroweak symmetry dynamically by chiral symmetry breaking among fermions (techniquarks) added to the standard model without its Higgs sector. This gives masses to the weak gauge bosons. The canonical way to also give masses to the standard model fermions is extended technicolor (ETC) [23]. In this context, the walking serves to relax the tension between the large mass of the top quark, which has to be generated, and the small bounds on flavor changing neutral currents, which have to be avoided. This is achieved by a sizable renormalization enhancement of the techniquark condensate. Apart from this primary purpose, extended technicolor may also stabilize the vacuum alignment [24] and make extra Nambu-Goldstone modes massive enough to avoid direct detection bounds. (Only three of the technipions serve as longitudinal modes of the weak gauge bosons.) The ramifications from extended technicolor are definitely already present before the techniquark condensate forms. Some of the effects connected to the stabilization of the vacuum alignment and the Nambu-Goldstone masses are similar in nature to an explicit mass term akin to the electroweakly induced quark masses relative to the chiral dynamics of quantum chromodynamics.

Therefore, in phenomenological applications the question after exact conformality is somewhat academic: The dynamics of ''pure'' technicolor are perturbed due to the coupling to the electroweak and extended technicolor. If the technipions are only to be removed outside detection bounds these modifications can be moderate or even altogether zero [25]. If, however, some of the technipions are to be heavy enough to serve as dark matter candidates, the modification is substantial. It is possible that these perturbations influence the amount of walking of a theory or even make a theory conformal, which otherwise would be exactly conformal.

As just discussed, in ''massless'' technicolor theories, walking is caused by intrinsically nonperturbative dynamics. As was already pointed out in [1], there is also the possibility to see walking from more perturbative effects: Consider an asymptotically free gauge theory that for massless flavors would feature an infrared fixed point but where some of the fermions have ''hard'' masses in analogy to the electroweak masses as seen by quantum chromodynamics. Then the infrared fixed point is never reached because the heavy fermions will freeze out for low energy scales, but, depending on the initial conditions, can be approached very closely. We are going to study this circumstance closely in what follows.

The plateau in the evolution of the coupling is the eponym for walking theories. The feature of importance for the construction of viable technicolor models is the renormalization of the mass operator of the fermions, $\int_{\mu_1}^{\mu_2} \frac{d\mu}{\mu} \gamma(\mu)$, where γ stands for the anomalous dimension of said operator and μ for the energy scale. Therefore, we will concentrate on this quantity.

The paper is organized as follows: Section II presents our mass-dependent all-order β function. Section III analyzes the interplay between quasiconformality and mass, where Sec. III A is concerned with the determination quasiconformal window. Section III B identifies and analyzes universal behavior in the vicinity of a would-be fixed point. Section III C puts our findings to use in the construction of walking technicolor models. Section IV summarizes the results.

II. β FUNCTIONS

The β function is defined as the change of the gauge coupling g of a field theory with the energy scale μ due to renormalization. In mass-independent subtraction schemes it is scheme independent up to two loops,

$$\beta(g) = -\frac{\beta_0}{(4\pi)^2} g^3 - \frac{\beta_1}{(4\pi)^4} g^5 - \cdots, \tag{1}$$

$$\beta_0 = \frac{11}{3} C_2(G) - \frac{4}{3} T(R) N_f, \tag{2}$$

$$\beta_1 = \frac{34}{3} C_2(G)^2 - \frac{20}{3} C_2(G) T(R) N_f - 4 C_2(R) T(R) N_f. \tag{3}$$

In the mass-dependent background field momentum subtraction scheme, the first two coefficients are given by [2]

$$\beta_0 \mapsto \bar{\beta}_0 = \frac{11}{3} C_2(G) - \frac{4}{3} T(R) \sum_{j=1}^{N_f} b_0(x_j), \tag{4}$$

$$\beta_1 \mapsto \bar{\beta}_1 = \frac{34}{3} C_2(G)^2 - T(R) \sum_{j=1}^{N_f} b_1(x_j), \tag{5}$$

where $x_j = -\mu^2/(4m_j^2)$ and the mass m_j of the fermion flavor j. Additionally,

$$b_0(x) = 1 + 3[1 - G(x)]/(2x), \tag{6}$$

which is gauge invariant [10]. Here $G(x) = (2y\ln y)/(y^2-1)$, $y = (\sqrt{1-1/x}-1)/(\sqrt{1-1/x}+1)$,

$$\begin{aligned} b_1(x) = {} & \frac{16(1-x^2)C_2(R) + (1+8x^2)C_2(G)}{6x^2(1-x)}\sigma(x) - \frac{2}{3x^2}(C_2(G) - 2C_2(R))I(x) + \frac{2}{3x}\tilde{I}_3^{(4)}(x)C_2(G) \\ & + [(1+3x-10x^2+12x^3)C_2(G) - 3(3-3x-4x^2+8x^3)C_2(R)]\frac{4}{3x}G(x)^2 \\ & - [(147-4x-100x^2+8x^3)C_2(G) + 168(1-x)C_2(R) + 6(9+4x)\ln(-4x)C_2(G)]\frac{1}{9x}G(x) \\ & + [(99+62x)C_2(G) + 12(11+3x)C_2(R) + 2(27+24x-2x^2)\ln(-4x)C_2(G)]\frac{1}{9x}, \end{aligned} \tag{7}$$

$$\sigma(x) = \{2\mathrm{Li}_2(-y) + \mathrm{Li}_2(y) + [\ln(1-y) + 2\ln(1+y) - (3/4)\ln y]\ln y\}(1-y^2)/y, \tag{8}$$

$$I(x) = 6[\zeta_3 + 4\mathrm{Li}_3(-y) + 2\mathrm{Li}_3(y)] - 8[2\mathrm{Li}_2(-y) + \mathrm{Li}_2(y)]\ln y - 2[2\ln(1+y) + \ln(1-y)]\ln^2 y, \tag{9}$$

$$\tilde{I}_3^{(4)}(x) = 6\zeta_3 - 6\mathrm{Li}_3(y) + 6\mathrm{Li}_2(y)\ln y + 2\ln(1-y)\ln^2 y, \tag{10}$$

$\zeta_3 = \zeta(3) = 1.202\,056\,9\cdots$, and $\mathrm{Li}_n(z)$ is the polylogarithm.

For N_f mass degenerate flavors, here, for simplicity, all transforming under the same representation of the gauge group, the modifications of $\bar{\beta}_0$ and $\bar{\beta}_1$ relative to β_0 and β_1 can be gathered in "numbers of active flavors,"

$$N_{f,0} = N_f b_0(x), \tag{11}$$

$$N_{f,1} = N_f b_1(x)/[(20/3)C_2(G) + 4C_2(R)]. \tag{12}$$

In both cases $N_{f,i} \to N_f$ for $m \to 0$ and $N_{f,i} \to 0$ for $m \to \infty$. Hence, the decoupling theorem [3] is satisfied. Further, while $N_{f,0}$ interpolates monotonously between the two limiting cases N_f and zero, which would be expected from a number of active flavors. $N_{f,1}$ does not and is, in general, not even positive for all values of x. Hence, the interpretation as active number of flavors is more appropriate for $N_{f,0}$ than it is for $N_{f,1}$. Additionally, these modified numbers of flavors can be given a gauge invariant meaning [10], which makes the question why there should be different numbers of active flavors in each term of the β function even more acute.

Exploiting two-loop universality in the massless case (an expansion to two loops of the following expression reproduces the universal two-loop coefficients), a massless all-order β function was conjectured in [11],

$$\beta(g) = -\frac{g^3}{(4\pi)^2}\frac{\beta_0 - \frac{2}{3}T(R)N_f\gamma(g^2)}{1 - \frac{g^2}{8\pi^2}C_2(G)(1 + 2\frac{\beta_0'}{\beta_0})}. \tag{13}$$

Here $\beta_0' = C_2(G) - T(R)N_f$ and $\gamma = -d\ln m/d\ln\mu$ stands for the anomalous dimension of the fermion mass operator. To universal massless one-loop order $\gamma(g^2) = (3/2)C_2(R)g^2/(4\pi^2) + O(g^4)$. Furthermore, (13) reproduces limiting cases in which the β function is known exactly like, for example, super Yang-Mills theory [12] or planar equivalence in a large-N_c limit [13].

In [1], our mass-dependent all-order β function was derived based on the following requirements: When expanded to two-loop order the β-function coefficients in the background field momentum subtraction scheme are to be reproduced. [Alternatively, we could have used the physical charge approach of Ref. [10] as the target. The outcome, however, is qualitatively and quantitatively close to that in the background field momentum subtraction scheme (see especially Fig. 2 in [10]) and in the latter the expressions can be handled analytically.] Further, in the massless limit the mass-dependent all-order β function is to coincide with the mass-independent all-order β function. This ensures also that the exactly known results from supersymmetry are reproduced. Finally, in the ultramassive limit it is to coincide with the pure Yang-Mills version of the mass-independent all-order β function. This implies that all terms involving the Casimir $C_2(R)$ have to be absorbed in the term involving the anomalous dimension. This resulted in the following mass-dependent β function:

$$\bar{\beta}(g) = -\frac{g^3}{(4\pi)^2}\frac{\bar{\beta}_0 - \frac{2}{3}T(R)\sum_{j=1}^{N_f}\bar{\gamma}(x_j)}{1 - \frac{g^2}{8\pi^2}C_2(G)(1 + 2\frac{\bar{\beta}_0'}{\bar{\beta}_0})}. \tag{14}$$

Here

$$\bar{\gamma}(x_j) = \frac{3}{2}\frac{g^2}{4\pi^2}\frac{1}{4}b_1(x_j)|_{C_2(G)\to 0} \tag{15}$$

and

$$\bar{\beta}'_0 = C_2(G) + T(R)\sum_{j=1}^{N_f}\left[\frac{2}{3}b_0(x_j) - \frac{1}{4}\frac{b_1(x_j)|_{C_2(R)\to 0}}{C_2(G)}\right].$$

It can be generalized to accommodate flavors that transform under different representations of the gauge group. Then it becomes

$$\bar{\beta}(g) = -\frac{g^3}{(4\pi)^2}\frac{\bar{\beta}_0 - \frac{2}{3}\sum_{j=1}^{N_f} T(R_j)\bar{\gamma}(x_j)}{1 - \frac{g^2}{8\pi^2}C_2(G)(1 + \frac{\bar{\beta}'_0}{\bar{\beta}_0})}. \tag{16}$$

Here

$$\bar{\beta}'_0 = C_2(G) + \sum_{j=1}^{N_f} T(R_j)\left[\frac{2}{3}b_0(x_j) - \frac{1}{4}\frac{b_1(x_j)|_{C_2(R)\to 0}}{C_2(G)}\right] \tag{17}$$

and R_j is the representation of the flavor j. At fixed coupling $\bar{\gamma}(x_j)$ goes to 0 for $x \to 0$ and to the massless value for $x \to -\infty$, which is also observed for the mass-dependent anomalous dimension in [5]. [As was discussed before in [1], this would still be the case if a factor $1 + O(g^2)$ was incorporated in $\bar{\gamma}$ and/or $\bar{\beta}'_0$. It would appear at third order and could be absorbed in a change of the renormalization scheme, which is already true in the massless case. Hence, if one wanted to accommodate a particular three-loop term, one could include such a factor and adjust the denominator accordingly, which would amount to a change of scheme. One particular massless scheme adapted for studies in the framework of holographic duals [26] was introduced in [27].]

III. QUASICONFORMALITY AND MASS

Strictly speaking, already the exactly supersymmetric β function constitutes "only" a relation between the β function and the anomalous dimension of the fermion mass operator, and the latter is not known to all orders. Therefore, we do not have a parametrization of the β function of the form $\beta = \beta(g)$ at our disposal. This circumstance is inherited by the supersymmetry-inspired massless and mass-dependent β functions.

A. The (quasi)conformal window

Despite our ignorance of the exact form of the anomalous dimension, the all-order β functions allow us to find the lower bound of the conformal window or, in the mass-dependent case, the quasiconformal window:

In Ref. [15], the lower bound of the conformal window in the $N_c - N_f$ plane was determined by equating the coupling at the Caswell-Banks-Zaks fixed point with the critical coupling [28] for the formation of a chiral condensate in the ladder-rainbow approximation to the Dyson-Schwinger equations.

In Ref. [11], Eq. (13) was used to determine the lower bound of the conformal window by setting it equal to zero while putting the value of the anomalous dimension to its critical value for the onset of chiral symmetry breaking. The ladder-rainbow approximation yields 1 as the critical value. The only known theoretically hard upper bound on the anomalous dimension, however, arises from the requirement of unitarity of the field theory and is 2. (This is a consequence of the fact that in a conformal field theory the dimension $3 - \gamma$ of all nontrivial spinless operators including that of the chiral condensate must be larger or equal to unity [29] to avoid negative norm states.) The lower bound for the conformal window must, hence, not lie at a lower number of flavors. (Duality arguments [30] also give indications for choosing the critical value for the anomalous dimension.) This method has also been used for gauge groups other than $SU(N)$ and for multiple representations [31,32]. The framework leads to a universal relation for the lower bound of the conformal window [33], $1 = \kappa 2N_f T(R)/C_2(G)$. In Ref. [33], this relation was found in the worldline formalism; the value $\kappa \approx 1/4$ was determined from matching to SQCD. For comparison, from Eq. (13), one finds $\kappa = (2 + \gamma)/11$. (A combination of the two results would yield $\gamma \approx 3/4$.) Analogous relations were also found in [34]. For studies in the framework of the renormalization group flow see Ref. [35].

In Ref. [1], we studied the influence of threshold effects due to finite—that is, neither formally zero nor infinite—fermion masses based on the mass-dependent all-order β function (14) by fixing the anomalous dimension to the two benchmark values from the massless study. In a theory, where all fermion masses are nonzero, they freeze out for scales far enough below this mass. As a consequence, we are then effectively left with a pure Yang-Mills theory, where the antiscreening from the gluons is uncompensated. Therefore, what is determined by applying the above-described formalism is the phenomenologically decisive minimal number of flavors above which the coupling develops a plateau, that is, walks. Thus, we talk of a quasiconformal window, which in the massless limit coincides with the conformal window. For nonzero masses, the lower bound of the quasiconformal window is shifted to a larger number of flavors. In the strictly massless case, the walking theories are found slightly below the lower edge of the conformal window; above the edge, the theory evolves into the fixed point. In the massive case, slightly below the lower bound of the quasiconformal window, there will also be at least some walking. We expect that the amount of walking—the range of scales of quasiconformal behavior—is determined by an interplay of the freezing out of the flavors due to the explicit mass and the onset of chiral symmetry breaking. (Independent of walking, a similar interplay between quark mass effects and chiral symmetry breaking exists in quantum chromodynamics for the strange quark.) For a number of flavors too far below this bound the theory never comes close to the would-be fixed point and does not exhibit any walking. For a number of

flavors above the lower bound of the quasiconformal window an asymptotically free theory approaches the fixed point very closely and stays in its vicinity until the flavors start freezing out gradually. Once the flavors are decoupled sufficiently, the coupling starts running again. (We are going to study this decoupling process below.) As a consequence, the position of the low-energy end of the plateau is not set by the initial conditions for the renormalization group evolution of the gauge coupling alone, but also by the value of the fermion masses. In Ref. [1] we have determined the quasiconformal windows for $SU(N_c)$, $Sp(2N_c)$, and $SO(N_c)$ gauge groups. The critical number of flavors obtained by setting the mass-dependent β function equal to zero at a fixed critical value γ_c of the anomalous dimension is given by

$$N_f = \frac{11}{2}\frac{C_2(G)}{T(R)}[\gamma_c + 2b_0(x)]^{-1}. \tag{18}$$

The modification due to the mass of the fermion is, hence, universal in the sense that it neither depends on the gauge group nor the representation. The latter is encoded in the fraction $C_2(G)/T(R)$, while the mass effect is contained in $b_0(x)$.

B. Universal evolution in the quasiconformal window

Here we extract further pieces of information on the evolution of quasiconformal gauge field theories from the mass-dependent all-order β function (14). As we do not know the exact expression for the anomalous dimension of the fermion mass operator, we cannot describe the renormalization group evolution for just any generic setup. There is, however, universal behavior in the vicinity of the would-be fixed point: Consider a theory inside the quasiconformal window, where the evolution has (almost) reached what would be the infrared fixed point in the complete absence of mass. In that case, the β function is almost zero, as is its numerator. (At the same time, the coupling g is nonzero and thus is the anomalous dimension. Hence, while the coupling is almost stationary—due to the small value of β—the mass still grows when we decrease the energy scale.) When we reduce the energy scale, massive flavors will (continue to) freeze out, which leads to an increase of $\bar{\beta}_0$. As a consequence, the β function becomes slightly more negative, which, in turn, makes the coupling g grow slowly with decreasing energy scale. For an anomalous dimension that is a growing function of the coupling g the β function becomes, thus, again less negative. Taking stock, we have two counteracting effects, one—the freezing out of flavors—which drives β to negative values, and a second—the slow increase of the anomalous dimension—which restores the β function to zero.

From the definition

$$\delta = \bar{\beta}_0 - \frac{2}{3}T(R)\sum_{j=1}^{N_f}\bar{\gamma}(x_j), \tag{19}$$

we get

$$\bar{\beta}(g) = -\frac{g^3}{(4\pi)^2}\frac{\delta}{1-\frac{g^2}{8\pi^2}C_2(G)(1+2\frac{\bar{\beta}_0'}{\bar{\beta}_0})}, \tag{20}$$

and, considering for the moment N_f mass degenerate flavors,

$$\bar{\gamma} = \frac{11}{2}\frac{C_2(G)}{T(R)N_f} - 2b_0 - \frac{3}{2}\frac{\delta}{T(R)N_f}. \tag{21}$$

For the freeze-out of a flavor as described by b_0 the switching zone spans 5 orders of magnitude. (This also means threshold effects are felt for energy scales, which are more than 100 times bigger than the mass of the fermions.) We expect that the growth of the anomalous dimension and, hence, the restoration of the β function to almost zero, is able to follow nearly ''adiabatically'' the very gradual freezing out of flavors over 4 to 5 orders of magnitude as described by b_0. This can at least be seen from the two-loop study depicted in Fig. 2: When switching off a flavor suddenly (left panel) the coupling deviates strongly from its fixed point values. If it is switched off gradually, as described by b_0 (right panel), the coupling is almost able to follow its fixed point value. As a consequence, δ will be small and positive in the second case. Hence, in the following, we will at first neglect δ and will determine the corrections arising from a finite δ afterwards. Thus, omitting δ for the moment, we are left with the differential equation

$$-\frac{d\ln m}{d\ln\mu} = \frac{11}{2}\frac{C_2(G)}{T(R)N_f} - 2b_0\left(\frac{m}{\mu}\right). \tag{22}$$

With b_0 from Eq. (6) an analytic integration is not possible. Therefore, we will use the approximation [10]

$$b_0 \approx (1+5m^2/\mu^2)^{-1}, \tag{23}$$

which deviates by at most $\approx 1\%$ from Eq. (6) over the entire range of scales, and find

$$(c-1)\ln\frac{\mu}{\mu_0} = \ln\frac{\frac{m_0}{\mu_0}}{\frac{m}{\mu}} + \frac{1}{c+1}\ln\frac{c-1+5(c+1)\frac{m^2}{\mu^2}}{c-1+5(c+1)\frac{m_0^2}{\mu_0^2}}, \tag{24}$$

where $c = \frac{11}{2}\frac{C_2(G)}{T(R)N_f}$. As the lower bounds of integration we choose the point where Eq. (18) is satisfied, that is, where the critical anomalous dimension is reached and chiral condensation sets in, such that $\frac{m_0^2}{\mu_0^2} = \frac{1}{5}(\frac{2}{c-\gamma_c} - 1)$.

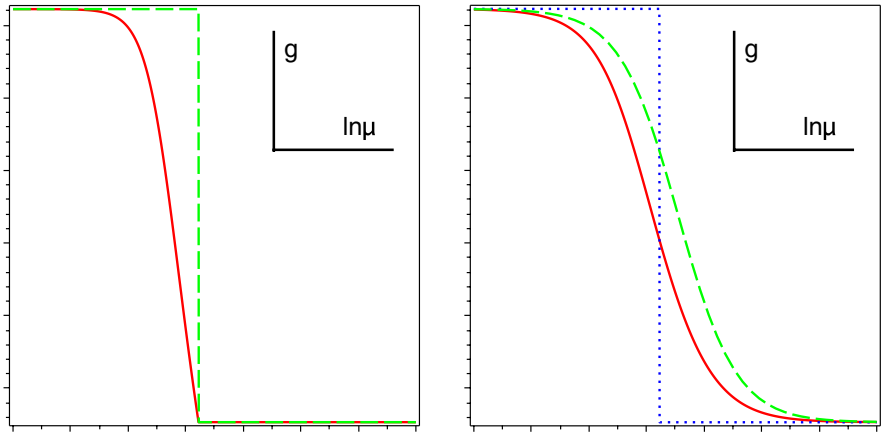

FIG. 2 (color online). Perturbative two-loop study of $g = g(\ln\mu)$ for the switching off of one flavor. Relaxation of the coupling g to the new fixed point value of the coupling (solid line, red). Fixed point value of the coupling for the active number of flavors at a given value of $\ln\mu$, $g[N_f(\ln\mu)]$ (dashed line, green). Left panel: sudden switching. Right panel: smooth switching; the blue dotted line serves to indicate twice the mass of the flavor.

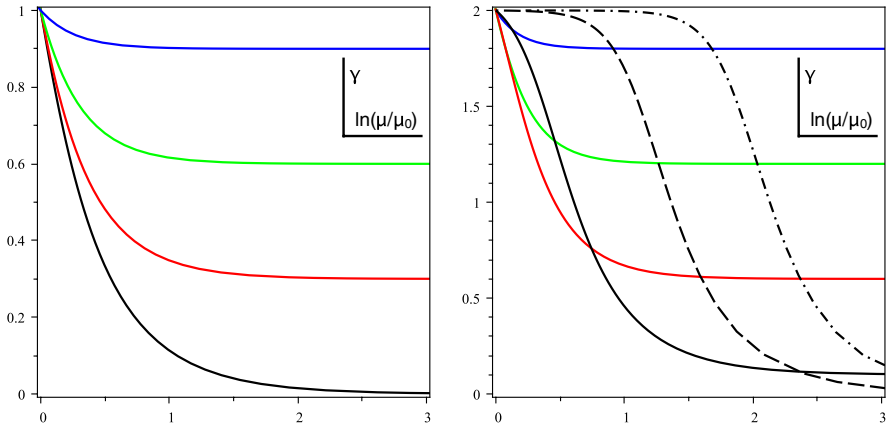

FIG. 3 (color online). Anomalous dimension as a function of the energy scale: Left panel, $\gamma_c = 1$; from top to bottom: $c = 2.9$ (blue line), $c = 2.6$ (green line), $c = 2.3$ (red line), $c = 2.0$ (black line). Right panel, $\gamma_c = 2$; from top to bottom, solid lines: $c = 3.8$ (blue), $c = 3.2$ (green), $c = 2.6$ (red), $c = 2.1$ (black); not solid lines, $c = 2.001$ (dashed), $c = 2.000\,01$ (dash-dotted).

Taking stock, Eq. (22) gives the anomalous dimension as a function of the ratio m/μ and Eq. (24) the scale μ as a function of the ratio m/μ. Hence, we are now in the position to plot the anomalous dimension as a function of the scale μ (see Fig. 3). For this we choose again the two customary benchmark values, where we set the critical anomalous dimension equal to 1 (left panel) or to 2 (right panel). We show the result for different values of $c \geq 2$, which is required for asymptotic freedom. On the left-hand side for all values of c and on the right-hand side for values of the parameter c far enough above 2, one sees the anomalous dimension comes from a plateau the position $(c - 2)$ of which is determined by the condition that the numerator of the β function vanish for all flavors active. Once the flavors start freezing out, the anomalous dimension starts increasing until the critical value for chiral condensation is reached. In the case where this critical value is 2, we see also a different behavior for values of c close to 2: A second plateau exists at the largest values of the anomalous dimension at the end of which the critical value is only just reached. (We will see more examples for this behavior below.) That such a kind of behavior can arise is linked to the fact that here we have to consider the limit $m/\mu \to \infty$ at fixed anomalous dimension and not fixed coupling. While the latter limit leads to the pure Yang-Mills result, the former leads to the result for $N_f/2$ flavors at $b_0 = 0$ in Eq. (22).

Further, we can also plot the logarithm of the mass renormalization factor, $\ln[m(\mu)/m(\mu_0)]$, as a function of the scale (see Fig. 4). As would be expected, the cases with pre-freeze-out plateau, where the plateau is at the largest value of the anomalous dimension, show the biggest renormalization factor for the mass. Their efficiency is, however, easily rivalled by those cases with a post-

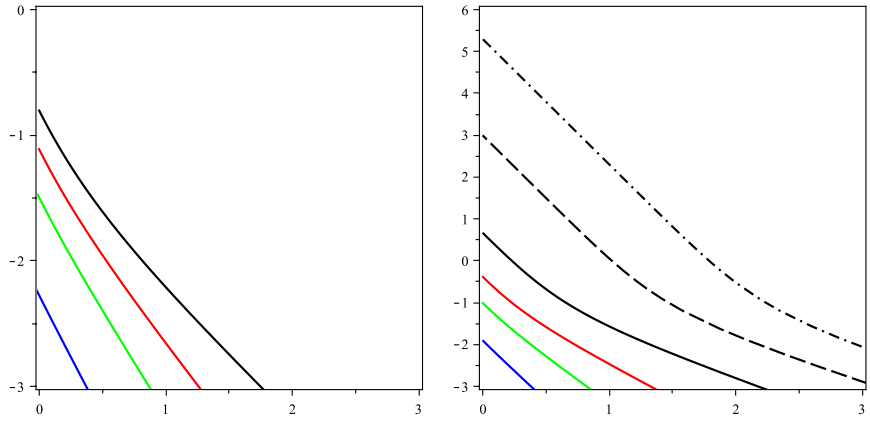

FIG. 4 (color online). Renormalization of the mass as a function of the energy scale. Left panel $\gamma_c = 1$; from bottom to top: $c = 2.9$ (blue), $c = 2.6$ (green), $c = 2.3$ (red), $c = 2.0$ (black). Right panel $\gamma_c = 2$; from bottom to top, solid lines: $c = 3.8$ (blue), $c = 3.2$ (green), $c = 2.6$ (red), $c = 2.1$ (black); $c = 2.001$ (dashed line), $c = 2.000\,01$ (dash-dotted line).

freeze-out plateau, where the anomalous dimension lingers very close to its critical value.

In order to determine the corrections from a finite δ, we invert Eq. (20) and get

$$\delta = -\frac{(4\pi)^2}{g^3}\left[1 - \frac{g^2}{8\pi^2}C_2(G)\left(1 + 2\frac{\bar{\beta}_0'}{\bar{\beta}_0}\right)\right]\frac{dg}{d\ln\mu} = 8\pi^2\frac{dg^{-2}}{d\ln\mu} + 2\frac{d\ln g}{d\ln\mu}C_2(G)\left(1 + 2\frac{\bar{\beta}_0'}{\bar{\beta}_0}\right). \tag{25}$$

Integrating and making use of the mean value theorem yields

$$\int_{\mu_1}^{\mu_2}\frac{d\mu}{\mu}\,\delta = \left[\frac{2\pi^2}{g^2} + \frac{1}{2}\ln(g)C_2(G)\left(1 + 2\left\langle\frac{\bar{\beta}_0'}{\bar{\beta}_0}\right\rangle\right)\right]_{g(\mu_1)}^{g(\mu_2)}, \tag{26}$$

where $\langle\bar{\beta}_0'/\bar{\beta}_0\rangle$ stands for $\bar{\beta}_0'/\bar{\beta}_0$ evaluated at an intermediate value of μ. If the anomalous dimension changes slowly, the β function remains very close to zero, $g(\mu_2)$ stays close to $g(\mu_1)$, and the deviation from our result is small. Where the anomalous dimension changes at a higher rate the logarithmic term leads to an enhancement of the mass renormalization and the g^{-2} term to a reduction. Hence, we can estimate,

$$\int_{\mu_1}^{\mu_2}\frac{d\mu}{\mu}\,\delta < \frac{8\pi^2}{[g(\mu_2)]^2} - \frac{8\pi^2}{[g(\mu_1)]^2} < \frac{8\pi^2}{[g(\mu_2)]^2}. \tag{27}$$

If we accept that for a given value of the coupling the full expression for the anomalous dimension is reduced relative to the one-loop result by the higher order terms, we get

$$\int_{\mu_1}^{\mu_2}\frac{d\mu}{\mu}\,\delta < \frac{8\pi^2}{[g(\mu_2)]^2} = 3\frac{C_2(R)b_0}{\gamma_{1\bigcirc}(\mu_2)} < 3\frac{C_2(R)b_0}{\gamma(\mu_2)}. \tag{28}$$

According to Eq. (21) the number that has to be compared to the renormalization factor of the mass is given by

$$\frac{3}{2}\int_{\mu_1}^{\mu_2}\frac{d\mu}{\mu}\,\frac{\delta}{T(R)N_f} < \frac{9}{2}\,\frac{C_2(R)b_0}{T(R)N_f\gamma(\mu_2)} \ll \int_{\mu_1}^{\mu_2}\frac{d\mu}{\mu}\,\bar{\gamma} < \bar{\gamma}(\mu_2)\ln\frac{\mu_2}{\mu_1}. \tag{29}$$

We are interested in theories with small N_c and N_f. This makes all quantities in the previous inequality $O(1)$ apart from the factor b_0. For large masses $m \gg \mu$ it becomes $b_0 \ll 1$. Hence, the previous very conservative estimate suffices to show that our computation is accurate not only in the post-freeze-out plateau but also in the part of the slope where $b_0 \ll 1$. For assessing the cases with pre-freeze-out plateaus the last estimate in Eq. (28) is too lavish. For a pre-freeze-out plateau, if the value of $\int(1 - b_0)d\ln\mu \ll 1$ one is on the safe side. All the way to the onset of chiral condensation this criterion is only satisfied for large values of c. (See, for example, the blue (top) lines in Fig. 3.)

But what is the effect of a finite δ? In regions of changing b_0 the effective value of c is reduced. The curves in the right panel of Fig. 3 get steeper as c becomes smaller. Hence, addressing a finite δ would generically steepen the slopes there more, while leaving the plateaus unchanged. The same holds for the red, green, and blue (nonblack) curves in the right panel. For the black curves, however, the effective reduction of c does not lead to any steeper slopes, but the post-freeze-out plateau is stabilized by the reduction of c.

1. Partially massive

Now let us generalize to the case with N_f massive and n_f massless flavors. Equation (19) becomes

$$\delta = \tfrac{11}{3}C_2(G) - \tfrac{2}{3}T(R)[N_f(2b_0 + \bar{\gamma}) + n_f(2 + \hat{\gamma})], \tag{30}$$

where $\hat{\gamma}$ is the anomalous dimension for the massless fermions. For a given value of the coupling g, the anoma-

lous dimension of the massive fermions is reduced relative to that of the massless fermions and at fixed coupling goes to zero in the limit of infinite masses. Defining the ratio between the two as $\hat{\gamma} = \bar{\gamma}/\hat{b}_0$ leads to the equivalent of Eq. (22),

$$\bar{\gamma} = \frac{11}{2}\frac{C_2(G)}{T(R)(N_f + n_f/\hat{b}_0)} - 2\frac{N_f b_0 + n_f}{N_f + n_f/\hat{b}_0}. \tag{31}$$

For b_0 and $\hat{b}_0$ close to unity, $b_0 = 1 - \epsilon$ and $\hat{b}_0 = 1 - \hat{\epsilon}$, that is, for small masses, we find

$$\bar{\gamma} \approx \frac{11}{2}\frac{C_2(G)}{T(R)(N_f + n_f)}\left(1 - \frac{n_f\hat{\epsilon}}{N_f + n_f}\right) \tag{32}$$

$$- 2\left(1 - \frac{N_f\epsilon + n_f\hat{\epsilon}}{N_f + n_f}\right). \tag{33}$$

For b_0 and $\hat{b}_0$ close to zero, that is, for large masses,

$$\bar{\gamma} \approx \left[\frac{11}{2}\frac{C_2(G)}{T(R)n_f} - 2\right]\hat{b}_0. \tag{34}$$

Hence, b_0 and $\hat{b}_0$ can only be small if the anomalous dimension for the massive flavors is small. In fact, the previous relation gives consistently the known fixed point value of the anomalous dimension for n_f massless flavors,

$$\hat{\gamma} \approx \frac{11}{2}\frac{C_2(G)}{T(R)n_f} - 2. \tag{35}$$

Expanding to the next order we get

$$\hat{\gamma} \approx \left(\frac{11}{2}\frac{C_2(G)}{T(R)n_f} - 2\right)\left(1 - \frac{N_f}{n_f}\hat{b}_0\right) - 2\frac{N_f}{n_f}b_0. \tag{36}$$

We notice that in Eq. (31), as is visible more directly in Eqs. (33) and (36), b_0 and $\hat{b}_0$ always act in the same direction; everywhere appear weighted sums of the two reduction factors and never differences. Therefore, the outcome is less sensitive to the exact form of b_0 relative to $\hat{b}_0$ as the general requirements are satisfied. Therefore, we use henceforth $\hat{b}_0 = b_0$. Thus,

$$\bar{\gamma} = \left[\frac{11}{2}\frac{C_2(G)}{T(R)(N_f b_0 + n_f)} - 2\right]b_0, \tag{37}$$

or

$$\hat{\gamma} = \frac{11}{2}\frac{C_2(G)}{T(R)(N_f b_0 + n_f)} - 2. \tag{38}$$

Hence, we can write the equivalent of Eq. (22) with b_0 from Eq. (23) as

$$d\ln\mu = \frac{-(1 + 5\frac{m^2}{\mu^2})[N_f + n_f(1 + 5\frac{m^2}{\mu^2})]d\frac{m}{\mu}/\frac{m}{\mu}}{(1 + 5\frac{m^2}{\mu^2})C - (1 - 5\frac{m^2}{\mu^2})[N_f + n_f(1 + 5\frac{m^2}{\mu^2})]}, \tag{39}$$

where $C = \frac{11}{2}\frac{C_2(G)}{T(R)}$. The integral can be carried out analytically but leads to a rather lengthy expression, which we choose not to display here. As the lower boundary of integration we choose the point where Eq. (38) equals the critical value of the anomalous dimension for which chiral condensation sets in, such that

$$5\frac{m_0^2}{\mu_0^2} = \left[\frac{11}{2}\frac{C_2(G)}{T(R)N_f}\frac{1}{\gamma_c + 2} - \frac{n_f}{N_f}\right]^{-1} - 1. \tag{40}$$

In the massless sector we get from $\hat{\gamma} = -d\ln\lambda/d\ln\mu$ using the chain rule,

$$\frac{d\ln\lambda}{d\ln\frac{m}{\mu}} = \frac{\hat{\gamma}}{1 + \bar{\gamma}}. \tag{41}$$

Making use of Eqs. (37) and (38), we obtain

$$\frac{d\ln\lambda}{d\ln\frac{m}{\mu}} = \frac{[b_0^{-1}(C - 2n_f) - 2N_f]b_0^{-1}}{n_f b_0^{-2} + (N_f - 2n_f + C)b_0^{-1} - 2N_f}, \tag{42}$$

which can be integrated analytically after making use of Eq. (23) and again yields a lengthy expression, which we choose not to display here.

After the above integrations, we are again in the position to display the anomalous dimensions for the massive and massless fermions as functions of the energy scale μ (see Fig. 5). For all choices of parameters, at high scales, where the masses of the massless particles are still comparatively small, the anomalous dimensions for both particle species coincide as they should. They are to be found in (pre-freeze-out) plateaus at the same value as in the fully massive case for the same value of the parameter c. Once the massive fermions start freezing out, their anomalous dimension is left behind by that of the massless fermions (dotted lines), which goes toward the critical value for the onset of chiral condensation. Usually, when the freeze-out begins, the anomalous dimension of the massive fermions will (at least at first) follow the increase of the anomalous dimension of the massless quarks. Only when there are more massless than massive quarks (see, for example, the case $n_f = 3N_f$ in the middle panel), the anomalous dimension of the massive fermions can also start decreasing immediately. If the critical anomalous dimension is reached sufficiently late in the freeze-out process of the massive fermions, their anomalous dimension will begin falling again. If the freeze-out is almost complete at the onset of chiral condensation, the anomalous dimension of the massive fermions goes to zero. This happens in those setups in which also a post-freeze-out plateau develops in the anomalous dimension of the massless fermions. Very importantly, in the partially massive case post-freeze-out plateaus in the anomalous dimension of the massless flavors appear also for a critical value of the anomalous dimension for chiral condensation of 1 (see the middle panel). It is no longer a special feature of the case where this value equals 2. Further, there can also be a pre-freeze-

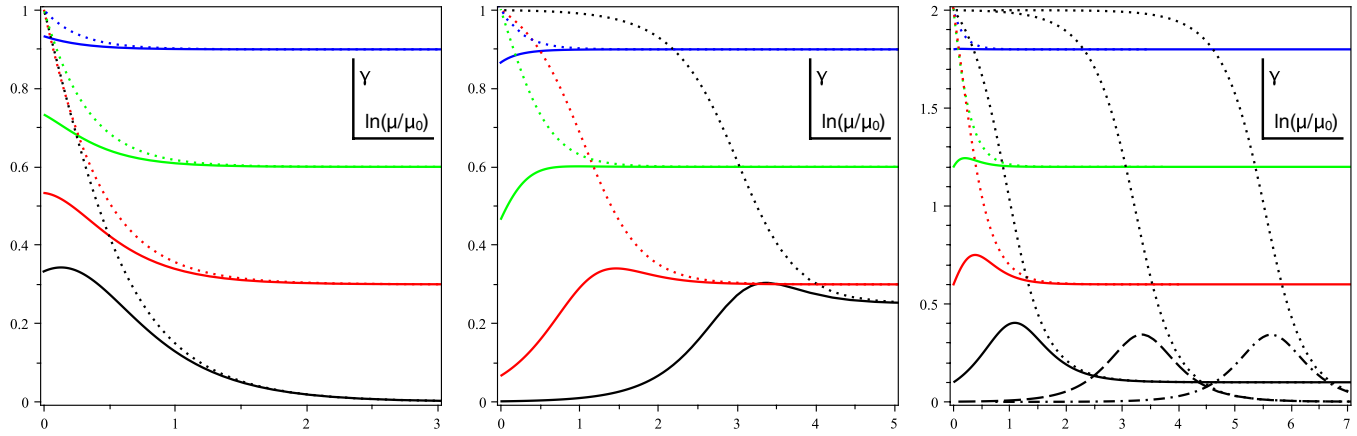

FIG. 5 (color online). Anomalous dimension of the massless (dotted lines) and massive (other lines) fermions as functions of the energy scale. The plateaus at high scales level out at $\gamma = c - 2$. Left panel: $\gamma_c = 1$, $N_f = n_f$; from top to bottom, $c = C/(N_f + n_f) = 2.9$ (blue), $c = 2.6$ (green), $c = 2.3$ (red), $c = 2.0$ (black). Middle panel: $\gamma_c = 1$, $3N_f = n_f$; from top to bottom, $c = 2.9$ (blue), $c = 2.6$ (green), $c = 2.3$ (red), $c = 2.251$ (black). Right panel: $\gamma_c = 2$, $N_f = n_f$; from top to bottom, $c = 3.8$ (solid blue), $c = 3.2$ (solid green), $c = 2.6$ (solid red), $c = 2.1$ (solid black); $c = 2.001$ (black dashed), $c = 2.000\,01$ (black dash-dotted).

out plateau at nonzero anomalous dimension (see the black curves in the middle panel). In this context, the larger the number of massless flavors as compared to the number of massive flavors, the larger is the value of the anomalous dimension in the pre-freeze-out plateau. This statement also holds in the case, where the anomalous dimension at the onset of chiral condensation equals 2.

Figure 6 displays the logarithms of the renormalization factors of the mass operators as a function of the logarithm of the scale prior to chiral condensation. The dotted lines are for the massless fermions, and the others for the massive ones. (Nearly) horizontal stretches correspond to small anomalous dimensions and steep stretches to large values of the anomalous dimension. The post-freeze-out plateaus are characterized by a maximally steep approach to the origin of the renormalization of the massless flavors. The achieved renormalizations generically exceed the renormalization achieved with a pre-freeze-out plateau. If a pre-freeze-out plateau is situated at a large value of the anomalous dimension it approaches the origin at an almost maximal slope and bends into the maximal slope (maximal anomalous dimension) just before finally meeting the origin.

Figure 7 presents the logarithm of the mass to scale ration as a function of the energy scale. Apart from the overall evolution of the ratio, the intercepts at the scale at which chiral condensation sets in are of particular interest. For situations with post-freeze-out plateau, these intercepts

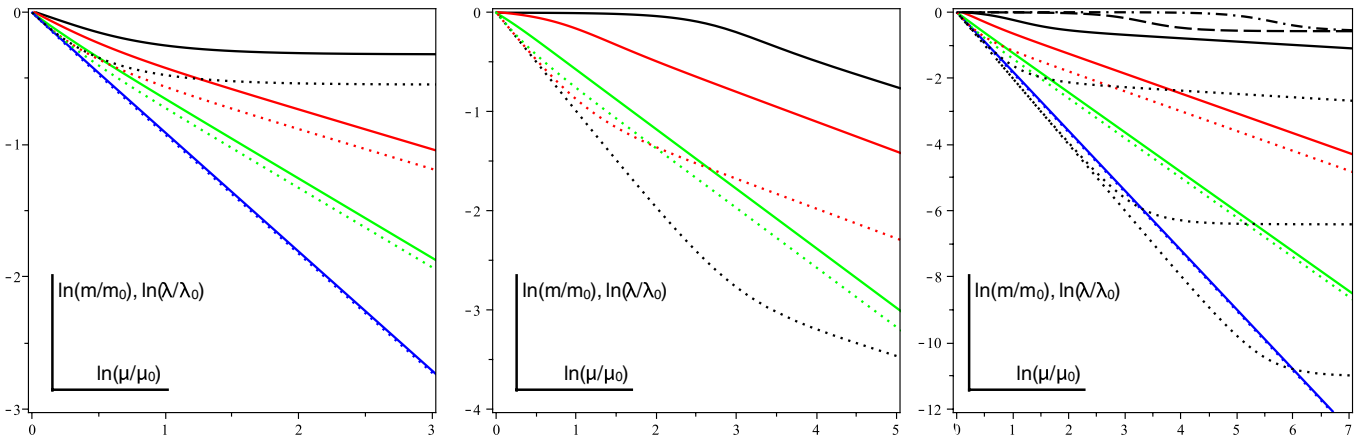

FIG. 6 (color online). Renormalization of the mass operators of the massless (dotted lines) and the massive (other lines) flavors. Left panel, $\gamma_c = 1$, $N_f = n_f$; from bottom to top, $c = 2.9$ (blue), $c = 2.6$ (green), $c = 2.3$ (red), $c = 2.0$ (black). Middle panel, $\gamma_c = 1$, $3N_f = n_f$; from top to bottom, $c = 2.9$ (blue), $c = 2.6$ (green), $c = 2.3$ (red), $c = 2.251$ (black). Right panel, $\gamma_c = 2$, $N_f = n_f$; from bottom to top, solid: $c = 3.8$ (blue), $c = 3.2$ (green), $c = 2.6$ (red), $c = 2.1$ (black); not solid: $c = 2.001$ (dashed), $c = 2.000\,01$ (dash-dotted).

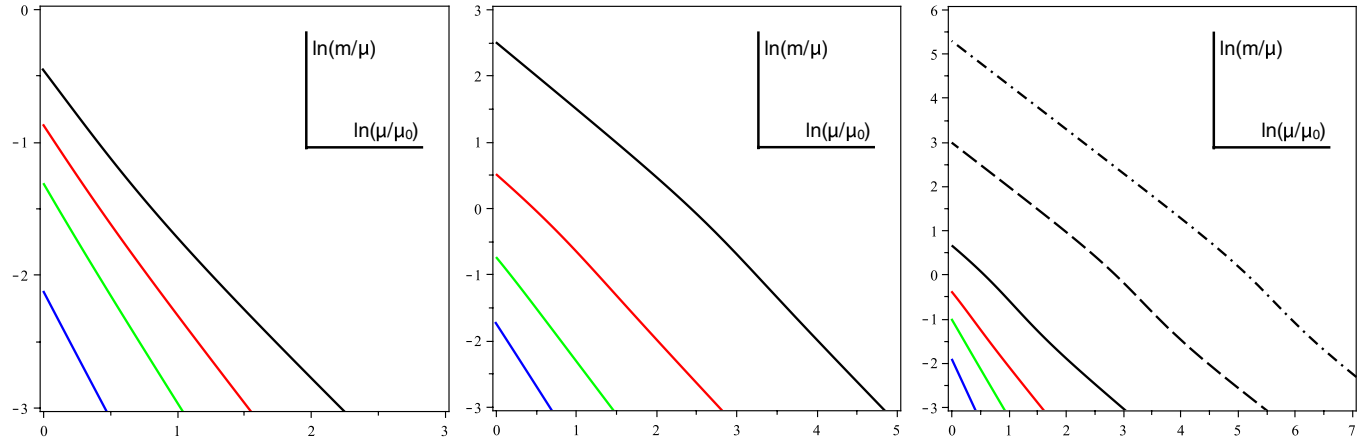

FIG. 7 (color online). Logarithm of the mass to scale ratio as a function of the energy scale. Left panel, $\gamma_c = 1$, $N_f = n_f$; from bottom to top, $c = 2.9$ (blue), $c = 2.6$ (green), $c = 2.3$ (red), $c = 2.0$ (black). Middle panel, $\gamma_c = 2$, $3N_f = n_f$; from bottom to top, $c = 2.9$ (blue), $c = 2.6$ (green), $c = 2.3$ (red), $c = 2.251$ (black). Right panel $\gamma_c = 2$, $N_f = n_f$; from bottom to top, solid: $c = 3.8$ (blue), $c = 3.2$ (green), $c = 2.6$ (red), $c = 2.1$ (black); not solid: $c = 2.001$ (dashed), $c = 2.000\,01$ (dash-dotted).

are especially large. That means that in these situations the renormalization group enhancement of the condensate of the massless fermions takes place, while the extra massive quarks are much heavier than the scale. To the contrary, for models with pre-freeze-out plateau the intercepts are small; the massive quarks are lighter than the energy scale at the onset of chiral condensation. At the same moment their anomalous dimensions are large as well, which implies that they also might partake in the chiral condensation process. If, in the limit of light massive quarks, we resort to the Gell-Mann–Oakes–Renner relation to estimate the masses of the pions incorporating one (''light-heavy pion'') or two (''doubly heavy pion'') of the massive flavors we find $m^2_{\pi_{\rm hl}} = 1m\langle Q\bar{Q}\rangle f_\pi^{-2}$ or $m^2_{\pi_{\rm hh}} = 2m\langle Q\bar{Q}\rangle f_\pi^{-2}$ where, in a technicolor setting, $\langle Q\bar{Q}\rangle = O\ (\mathrm{TeV}^3)$ and $N_f^{\rm cond} f_\pi^2 = 2\Lambda_{\rm ew}^2$. $N_f^{\rm cond}$ is the number of flavors participating in the condensation process. From there we get $(m_{\pi_{\rm hl}}/\mathrm{TeV})^2 = 8N_f^{\rm cond} \times (m/\mathrm{TeV})$. For the smallest intercept in the right panel of Fig. 7 of $(m/\mathrm{TeV}) \lesssim -2$ this yields $m_{\pi_{\rm hl}}/\mathrm{TeV} \approx (N_f^{\rm cond})^{1/2}$.

Deviations from the present analysis arise from the term $-\frac{3}{2}\frac{1}{T(R)}\frac{\delta}{(N_f+n_f/b_0)}$. Hence, we have to study

$$\int_{\mu_1}^{\mu_2} \frac{d\mu}{\mu}\frac{\delta}{\tilde{N}_f} = \left[\frac{8\pi^2}{g^2}\langle\tilde{N}_f^{-1}\rangle + 2\ln(g)C_2(G)\left\langle\frac{1+2\frac{\bar{\beta}_0'}{\bar{\beta}_0}}{\tilde{N}_f}\right\rangle\right]_{g(\mu_1)}^{g(\mu_2)}, \quad (43)$$

where $\tilde{N}_f = N_f + n_f/b_0$. $\langle\cdots\rangle$ again indicates an intermediate value in the sense of the mean value theorem. If the anomalous dimension changes slowly, the β function remains close to zero, $g(\mu_2)$ stays close to $g(\mu_1)$, and the deviation from our result is small. Where the anomalous dimension changes at a higher rate the logarithmic term leads to an enhancement of the mass renormalization and the g^{-2} term to a reduction. We can estimate once more,

$$\int_{\ln\mu_1}^{\ln\mu_2} d\ln\mu\,\frac{\delta}{\tilde{N}_f} < \langle\tilde{N}_F^{-1}\rangle\frac{8\pi^2}{[g(\mu_2)]^2} = \langle\tilde{N}_F^{-1}\rangle 3\frac{C_2(R)}{\hat{\gamma}_{1\bigcirc}(\mu_2)} < \langle\tilde{N}_F^{-1}\rangle 3\frac{C_2(R)}{\hat{\gamma}(\mu_2)}. \quad (44)$$

For an analysis in the range of large masses, $\langle\tilde{N}_F^{-1}\rangle \approx \langle b_0/n_f\rangle$. As there $b_0 \ll 1$, large masses further reduce the deviation. As in the previous fully massive case this shows that the behavior in the vicinity of the post-freeze-out plateau is well captured in the present approximation. Around the pre-freeze-out plateau the accuracy is again assured while the value of $\int(1-b_0)d\ln\mu$ as integrated backward from the plateau toward smaller values of the scale remains small compared to unity.

In areas where b_0 is changing, that is, for finite δ, the effective value of C is reduced. For the curves depicting the anomalous dimensions for the massless flavors in the left panel of Fig. 5 this will lead to a steepening in the freeze-out region, as seen above in the fully massive case. At the larger values of the parameter C this also holds for the anomalous dimensions of the massive particles. At smaller values the flattening out and, ultimately, the relative maximum seen in the black curve could become visible due to the shift in the effective value of C. For the middle panel the steepened increase of the anomalous dimension of the massless fermions persists for the larger values of C. There, the anomalous dimension of the massive flavors is falling and the rate of this falloff is also increased by an effective reduction of C. For smaller values of the parameter C an effective reduction tends to introduce a small local

maximum and afterward a falloff down to zero into the curves for the anomalous dimension of the massive fermions. In the curve for the massless flavors a post-freeze-out plateau is introduced and stabilized. The slope connecting the pre- to the post-freeze-out plateau is universal and should not be affected. What has been said here about the curves in the middle panel holds also for the right panel: For large values of C an effective reduction of C in the freeze-out region steepens the approach of the anomalous dimension of the massless fermions to the critical value of the anomalous dimension; for smaller values the post-freeze-out plateau is stabilized. For the massive flavors first a maximum is introduced (at larger C) and then a drop down to vanishing anomalous dimensions, while the maximum (seen at smaller C) is pushed to the left.

2. Outlook I

One possible generalization of what has been discussed here so far could address systems with more than two different types of flavors characterized by their mass. The lightest flavors will always set the boundary condition because their anomalous dimension will always reach the critical value first. The fermions for which the number of active flavors changes most in the interesting range of scales would influence the dynamics most.

Because of what is perceived as a relatively small matter content, one commonly does not expect quantum chromodynamics to be close to a fixed point in the renormalization group evolution when chiral symmetry is breaking. Hence, the present analysis, which is based on the nearness of a would-be fixed point should receive important corrections. One does not expect any plateaus, neither pre- nor post-freeze-out. The pattern of two light flavors (u and d) in conjunction with one flavor (s) that is actively freezing out at the scale where chiral symmetry breaks is, however, reminiscent of what has been discussed above. (Actually, according to the description of the effective number of active flavors the c and even the b quark are not fully frozen out, while the t quark is to a better approximation infinitely massive than the u and d are massless.) As a consequence, if the dynamics of chiral symmetry breaking in quantum chromodynamics should be dominated by the freeze-out of the s quark, the universal slope in the freeze-out curves might play a role even there, in the sense that the final approach of the anomalous dimension of the u and the d quark looks like the upper end of the black dotted curve in the right panel of Fig. 5 and possibly continues steeper down to perturbatively small values. (The s quark could not play such a potential important role in this context if it were not provided with a fitting explicit mass by the breaking of the electroweak symmetry.)

Another extension could deal with fermions with different representations on top of different masses, as the massive all-order β function (14) also allows for fermions in different representations to be present simultaneously. This requires information on the relationship between the anomalous dimensions of the flavors transforming under different representations.

3. Outlook II: Enhanced flavor symmetry

For a moment, let us consider technicolor models with two flavors. (Concrete models are realized in the form of minimal and next-to-minimal walking technicolor [18,19,36].)

Such theories with techniquarks in non-(pseudo)real representation of the technicolor gauge group feature an $SU(2)_L \times SU(2)_R \to SU(2)_V$ chiral symmetry breaking pattern. It entails always the correct breaking of the electroweak symmetry, $SU(2)_L \times U(1)_Y \to U(1)_{\rm em}$ [24].

For techniquarks in a strictly real representation the breaking pattern is $SU(4) \to SO(4)$. Electroweak radiative corrections provide the 6 Nambu-Goldstone bosons that do not become the longitudinal degrees of freedom of the weak gauge bosons with positive squared masses, which stabilizes the correct vacuum alignment [24] and takes them beyond the direct exclusion limit for technipions [25,37].

For a pseudoreal representation the breaking pattern is $SU(4) \to Sp(4)$ with two extra technipions, which receive negative contributions to their squared masses from electroweak radiative corrections, which, in turn, destabilizes the correct embedding. This has to be counteracted by an appropriate mechanism (extended technicolor).

All it takes to break the electroweak symmetry appropriately is an $SU(2)_L \times SU(2)_R \to SU(2)_V$ chiral symmetry breaking pattern. Hence, above the technicolor scale not the full $SU(4)$ symmetry needs to be preserved, but merely the $SU(2)_L \times SU(2)_R$ subgroup: The pure two-flavor technicolor sector is made up of 4 Weyl fermions, which can be collected in a column vector

$$\begin{pmatrix} U_L \\ D_L \\ -i\sigma^2 U_R^* \\ -i\sigma^2 D_R^* \end{pmatrix}$$

in which all components transform as left fields. This makes the $SU(4)$ flavor symmetry more obvious. What is called left and what right is determined by the way the electroweak sector is coupled in. For the flavor symmetry the mass terms

$$\mathcal{L}_m = m(\bar{U}_L U_R + \bar{U}_R U_L + \bar{D}_L D_R + \bar{D}_R D_L) \tag{45}$$

and

$$\mathcal{L}_\lambda = \lambda(\bar{U}_L D_L + \bar{D}_L U_L + \bar{U}_R D_R + \bar{D}_R U_R) \tag{46}$$

are equivalent. They can be expressed by contracting two of the above column vectors with the matrices

$$\begin{pmatrix} \mathbb{0} & \mathbb{1} \\ \mathbb{1} & \mathbb{0} \end{pmatrix} \quad \text{or} \quad \begin{pmatrix} \mathbb{1} & \mathbb{0} \\ \mathbb{0} & -\mathbb{1} \end{pmatrix}. \tag{47}$$

$\mathbb{0}$ and $\mathbb{1}$ stand for 2×2 zero and unit matrices, respectively.

Only the first mass term breaks the electroweak symmetry. The second leaves a residual $SO(4) \simeq SU(2)_L \times SU(2)_R$ flavor symmetry behind. It contributes to the masses of the Nambu-Goldstone bosons that correspond to generators that link left with right fields. (These are the modes with finite technibaryon number.) For techniquarks in a pseudoreal representation of the technicolor gauge group, terms which break the $SU(4)$ flavor symmetry to $SU(2)_L \times SU(2)_R$ are needed to stabilize the vacuum. Another motivation for studying the interplay between an explicit $\mathcal{L}_\lambda$ mass term with a chiral condensation taking place in the $\mathcal{L}_m$ channel is to regulate the amount of walking of the theory or to circumvent the exact conformality of a given setup [38]. As opposed to the partially massive case analyzed in detail above, where the massive and massless fields are clearly separated, the last mentioned case with $\mathcal{L}_\lambda$ and $\mathcal{L}_m$ channels does not allow for such a clear separation of the fields. Therefore, a corresponding treatment in the present framework requires further study.

C. Use in constructing walking technicolor models

Walking dynamics in technicolor theories serve to relieve the tension between the large mass of the top quark, which has to be generated by extended technicolor interactions, and the small experimental bounds on flavor changing neutral currents, by a sizable renormalization of the techniquark condensate. With all flavors exactly massless these models are to be found just below the conformal window in the $N_c - N_f$ plane. Here the approach is slightly different from massless walking technicolor, as we are considering theories that would be inside the conformal window and would thus evolve into an infrared fixed point, if all their techniquarks were massless. We regard instead a theory where at least two flavors are massless and gauged under the electroweak. This assures that the electroweak symmetry is not broken explicitly before the chiral symmetry is broken spontaneously. (Already in theories with all fermion massless and more than two flavors it is advantageous to gauge only two of them: Doing so makes it easier to avoid experimental bounds on the oblique parameters and solves the vacuum alignment problem, if the representation of the two gauged flavors does not happen to be pseudoreal [24]. These are the so-called partially gauged technicolor models introduced in [18].) In order to have an efficient renormalization enhancement of the techniquark condensate the anomalous dimension of the massless flavors has to stay close to a large value—optimally, close to its critical value—for a sizable range of energy scales before chiral condensation sets in. The above analysis indicates that this can be achieved in two different ways in the present context, by exploiting the pre-freeze-out plateau or the post-freeze-out plateau. In theories with pre-freeze-out plateau, the mass of the massive fermions is small compared to the energy scale. In theories with post-freeze-out plateau, the mass of the massive fermions is large compared to the energy scale. Hence, in the latter case, we have walking at maximal anomalous dimension with heavy massive fermions as opposed to walking at almost maximal anomalous dimension with light massive fermions.

Massless walking technicolor theories have their number of flavors outside the conformal window, but as close as possible to the lower bound of the latter.

In theories with a pre-freeze-out plateau the total number $n_f + N_f$ of flavors is just inside the would-be conformal window. This is because, for the renormalization of the mass operator of the massless flavors to be as efficient as possible, the plateau value of the anomalous dimension of the mass operator of the massless techniquarks must be as close as possible to the critical value for the onset of chiral condensation as possible, and this is achieved by being just inside the would-be conformal window. The number n_f of massless fermions must be at least 2, to accommodate the dynamical electroweak symmetry breaking. Other than that, it is probably most advantageous to take all other flavors massive for reasons of vacuum alignment and direct discovery limits, for example, for extra Nambu-Goldstone modes. The presence of a pre-freeze-out plateau at a value of the anomalous dimension close to the critical is a generic feature in the sense that it is present for most gauge groups where the conformal window starts above 2 flavors (the minimal number we keep massless) and asymptotic freedom is not lost for 3 flavors (at least one additional massive flavor). This can be seen in the two last columns of Table I, which lists all theories based on $SU(N_c)$ gauge groups, which for two electroweakly gauged flavors have a sufficiently small contribution to the perturbative S_{pert} parameter. (Available electroweak precision data tell us that the S parameter should be small. In walking theories its perturbative value is a conservative upper estimate for its value.) In most cases the anomalous dimension is close to the critical value and leads thus to an efficient renormalization of the techniquark condensate.

In theories with a post-freeze-out plateau, the number n_f of massless flavors must be just outside the would-be conformal window. The total number $n_f + N_f$ of techniquarks can, in principle, be as large as allowed by asymptotic freedom. A number of only $N_f = 1$ massive flavors has the advantage of leading to a transition which is as smooth as possible, which extends the plateau. Further, this choice also features a pre-freeze-out plateau with optimal plateau value for the anomalous dimension for the massless techniquarks. Lastly, due to the thus most gradual transition, the here used approximations are under the best

TABLE I. List of all $SU(N)$ theories with a small perturbative S parameter. ($\pi S_{\rm pert} \leq 1$ when only two flavors are gauged.) The two benchmark values, 1 and 2, for the critical value of the anomalous dimension at which chiral condensation sets in, are analyzed. R stands for the representation (F = fundamental, G = adjoint, S = two-index symmetric, A = two-index antisymmetric), $N_f^{\gamma_c=2}$ ($N_f^{\gamma_c=1}$) for the lower bound of the conformal window if the critical value of the anomalous dimension for the onset of chiral condensation equals 2 (1), and $N_f^{\rm a.f.}$ for the total number of flavors above which asymptotic freedom is lost. The column marked by $\gamma_{\rm plateau}^{\gamma_c=2}$ ($\gamma_{\rm plateau}^{\gamma_c=1}$) shows the value of the anomalous dimension in the pre-freeze-out plateau for a total number of flavors that is just inside the would-be conformal window.

R	N_c	$\pi S_{\rm pert}$	$N_f^{\gamma_c=2}$	$N_f^{\gamma_c=1}$	$N_f^{\rm a.f.}$	$\gamma_{\rm plateau}^{\gamma_c=2}$	$\gamma_{\rm plateau}^{\gamma_c=1}$
F	2[a]	0.3	5.5	7.3	11.0	1.7	0.8
F	3[b]	0.5	8.3	11.0	16.5	1.7	0.8
F	4	0.7	11.0	14.7	22.0	1.7	0.9
F	5[b]	0.8	13.8	18.3	27.5	1.9	0.9
F	6	1.0	16.5	22.0	33.0	1.9	0.9
G	2[b]	0.3	1.4	1.8	2.8	[c]	[c]
G	3	0.7	1.4	1.8	2.8	[c]	[c]
S[d]	3	1.0	1.7	2.2	3.3	[c]	0.2
A[e]	4[f]	1.0	5.5	7.3	11.0	1.7	0.8

[a] $F2$ is a pseudoreal representation; the vacuum alignment has to be taken care of.
[b] A Witten anomaly has to be removed.
[c] $N_f^{\gamma_c=\bullet} < 2$.
[d] $S2$ coincides with $G2$.
[e] $A3$ coincides with $F3$.
[f] Apart from $S_{\rm pert}$ values for $A4$ coincide with values for $F2$.

possible control. The appearance of theories with a post-freeze-out plateau is less generic than that of theories with a pre-freeze-out plateau. It depends on how far the next integer number of flavors is below the edge of the conformal window. (This is a feature this phenomenon has in common with the massless technicolor theories [15].) The phenomenon can, however, be seen without fine-tuning, but by simply sticking to our benchmark values for the critical anomalous dimension and looking at various possible setups. In order to see this, consider the $SU(N_c)$ theories depicted in Fig. 8. The left panel features theories based on an $SU(3)$ technicolor group analyzed with the critical anomalous dimension equal to 1. The red and black curves (merging in the upper right quadrant) are for theories just inside the conformal window ($n_f + N_f = 12$). For any split of this number, there is a pre-freeze-out plateau. For the minimal number of massive flavors ($N_f = 1$) there is additionally a post-freeze-out plateau. In fact, for the plot the parameters were detuned slightly to allow the representation in a single panel, as for the exact choice of parameters, the post-freeze-out plateau becomes infinitely long. For the blue and green (i.e., the remaining) curves, the maximally allowed number of flavors allowed by asymptotic freedom ($N_f + n_f = 16$) has been chosen. For all possible splits of this number between massive and massless flavors, there is a pre-freeze-out plateau, but only at a very small value of the anomalous dimension. For the maximally allowed number of massless flavors for which the theory is not exactly conformal ($n_f = 11$) we see again a post-freeze-out plateau (which again has been

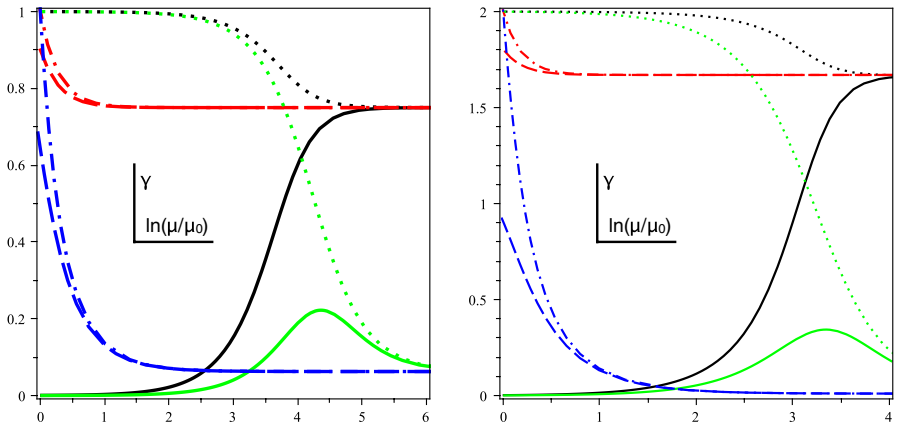

FIG. 8 (color online). Anomalous dimension as a function of the energy scale for different setups within the same technicolor gauge group. Left panel, $\gamma_c = 1$, gauge group $SU(3)$: black and red $N_f + n_f = 12$ (just inside conformal window); black $N_f = 1$ (minimal number of massive flavors), solid anomalous dimension of the massive flavor, dashed anomalous dimension of the massless flavors; red $n_f = 2$ (minimal number of massless flavors), dashed anomalous dimension of massive flavors, dash-dotted anomalous dimension of the massless flavors; green and blue $N_f + n_f = 16$ (just asymptotically free); green $n_f = 11$ (maximal number of massless flavors), solid anomalous dimension of the massive flavors, dotted anomalous dimension of the massless flavors; blue $n_f = 2$ (minimal number of massless flavors), dashed anomalous dimension of the massive flavors, dash-dotted anomalous dimension of the massless flavors. Right panel, $\gamma_c = 2$, gauge group $SU(4)$: everything is exactly the same as for the left panel, only for green and blue $N_f + n_f = 22$ (just asymptotically free). In both cases the length of the post-freeze-out plateaus (if present) has been shortened below the actual length to allow a representation in a single plot by detuning the parameters away from the actual values.

shortened by detuning). We do not see such a plateau if we only retain the minimal number ($n_f = 2$) of massless flavors that are required to construct a model of dynamical electroweak symmetry breaking. Analogous findings are displayed in the right panel for an $SU(4)$ model in the fundamental representation and analyzed with the critical anomalous dimension set to 2: Small total numbers of flavors lead to a more useful pre-freeze-out plateau and large numbers of massless flavors make it more likely to find a post-freeze-out plateau.

IV. SUMMARY

Here we have further analyzed the implications from the mass-dependent all-order β function derived in [1]. There it had already been used to determine the lower bound of the quasiconformal window. Here we proceed to identify universal behavior of the renormalization group evolution in the vicinity of a would-be fixed point and to shed more light on what is to be understood under the quasiconformal window (''would be'' because the evolution would hit the fixed point in the absence of masses). We analyze the cases where all fermions are massive and, phenomenologically more relevant, where part of them are massless prior to spontaneous chiral symmetry breaking. (In the partially massive case we rely on the assumption that the anomalous dimension for the fermion mass operator at fixed coupling and energy scale is a decreasing function of the fermion mass. In all cases we took the anomalous dimension as an increasing function of the coupling.) In both cases, we identify two kinds of walking behavior in the anomalous dimension as a function of the energy scale. In one case the plateau is ended (lowest energy scale) by the onset of the freeze-out of the massive fermions. The critical value of the anomalous dimension for the onset of chiral symmetry breaking is reached in the first half of the freeze-out process. Where the plateau starts (highest energy scale) depends on the initial condition for the renormalization group evolution. In the other case, the plateau begins when the massive flavors cannot freeze out much more, and it ends when the critical value of the anomalous dimension is finally reached. (The technical reason why this second type of plateau can arise also when all flavors have the same mass is, in short, that in the course of the analysis the mass has to be taken to infinity for fixed anomalous dimension and not for fixed coupling.) For a pre-freeze-out plateau the critical anomalous dimension is reached when the massive flavors are much lighter than the energy scale. Then also their anomalous dimension is not much below the value of the massless fermions and all flavors may participate in chiral condensation. For a post-freeze-out plateau the massive flavors are much heavier than the energy scale. Both plateaus can be present simultaneously and they can appear for any value of the critical anomalous dimension. (This is reminiscent of the situation identified for quantum chromodynamics in [39].)

In walking technicolor theories the tension between the generation of the large mass of the top quark by ETC interactions and the measured smallness of flavor changing neutral currents is alleviated by a renormalization enhancement of the techniquark condensate. In order for this process to be effective, the anomalous dimension of the mass operator of the techniquarks contributing to the chiral condensate has to be large (as close as possible to the critical value) for a sizable range of scales. The usual massless walking technicolor is constructed from massless techniquarks. Their total number must be as close as possible to the lower bound of the conformal window but outside. When allowing also for massive quarks the total number can also be inside the conformal window, only asymptotic freedom should of course not be lost. This opens the aisle for the construction of (partially) massive walking technicolor models where a freeze-out of one or several massive techniquarks in the vicinity of a would-be fixed point provides for the walking behavior. In this context it shows that such technicolor models with a pre-freeze-out plateau are rather generic in the sense that as long as the choice of gauge group and representation allows us to accommodate at least two massless techniquarks below the conformal window and at least a third massive techniquark without losing asymptotic freedom, we find mostly at least one combination of massive and massless fermions which lets the theory walk in a pre-freeze-out plateau not too far below the critical value of the anomalous dimension (see Table I). Theories with a post-freeze-out plateau are less generic, but can be found without fine-tuning. There the amount of walking depends on how far the next integer number of flavors is away from the critical number of flavors delimiting the conformal window. This is a feature they share with massless walking technicolor models.

Given the persisting uncertainty in the determination of the lower bound of the conformal window, the present findings also allow us to more smoothly interpolate between models. Before, given the critical value for the anomalous dimension, a model was either an appropriate candidate for a viable walking technicolor theory or it did not have the required features. Now, in the same situation, the value of γ_c sets limits on the masses of the massive fermions. For an especially striking example, compare the setups presented in green and blue, respectively (which enter the figure on the lower right-hand corner) in the right panel of Fig. 8. They have the same total number of flavors and as a consequence the same pre-freeze-out plateau value for the anomalous dimension, which happens to be too small for building a viable walking technicolor theory out of this setup. The green setup, featuring a pronounced splitting between massive and massless flavors, however, features also a post-freeze-out plateau, which makes it a candidate theory. The extrapolation from the pre-freeze-out plateau would have ruled out both combinations as viable candidates.

In this paper we have studied models with two types of techniquarks, one set of massless ones and another of mass degenerate massive ones. Another extension involves techniquarks in different simultaneously present representations, which can also be treated in the framework of the massive all-order β function [1]. Yet another extension would be to extend the construction of models to allow for Weyl flavors in places and not only Dirac flavors. An additional motivation for the present and the previous study was also to get an idea of effects, which are caused by the fact that realistically we are not dealing with idealized technicolor, but with technicolor, where the flavor symmetry is broken by the coupling to the electroweak sector or by extended technicolor, which either has to ascertain the correct vacuum alignment, that extra technipions escape direct detection, or, which probably leads to the strongest correction, that they are heavy enough to be viable candidates for cold dark matter. It might even be extended technicolor effects that make a theory quasiconformal, which from its bare technicolor structure would be completely conformal and hence, not suited for breaking the electroweak symmetry dynamically.

ACKNOWLEDGMENTS

The author would like to thank A. Armoni, R. Barbieri, J. Braun, S. J. Brodsky, M. Järvinen, F. Sannino, K. Socha, and A. I. Vainshtein for discussions. The work of D. D. D. was supported by the Danish Natural Science Research Council.

[1] D. D. Dietrich, Phys. Rev. D **80**, 065032 (2009).
[2] F. Jegerlehner and O. V. Tarasov, Nucl. Phys. **B549**, 481 (1999).
[3] T. Appelquist and J. Carazzone, Phys. Rev. D **11**, 2856 (1975).
[4] A. De Rujula and H. Georgi, Phys. Rev. D **13**, 1296 (1976).
[5] H. Georgi and H. D. Politzer, Phys. Rev. D **14**, 1829 (1976).
[6] O. Nachtmann and W. Wetzel, Nucl. Phys. **B146**, 273 (1978); D. A. Ross, Nucl. Phys. **B140**, 1 (1978).
[7] D. V. Shirkov, Teor. Mat. Fiz. **93**, 466 (1992) [Theor. Math. Phys. **93**, 1403 (1992)].
[8] J. Chyla, Phys. Lett. B **351**, 325 (1995).
[9] B. S. De-Witt, *A Gauge Invariant Effective Action, in Quantum Gravity II*, edited by C. J. Isham, R. Penrose, and D. W. Sciama (Oxford University Press, New York, 1981), pp. 449–487; L. F. Abbott, Nucl. Phys. **B185**, 189 (1981); A. Rebhan, Z. Phys. C **30**, 309 (1986).
[10] S. J. Brodsky, M. Melles, and J. Rathsman, Phys. Rev. D **60**, 096006 (1999).
[11] T. A. Ryttov and F. Sannino, Phys. Rev. D **78**, 065001 (2008).
[12] V. A. Novikov, M. A. Shifman, A. I. Vainshtein, and V. I. Zakharov, Nucl. Phys. **B229**, 381 (1983); D. R. T. Jones, Phys. Lett. **123B**, 45 (1983).
[13] A. Armoni, M. Shifman, and G. Veneziano, Nucl. Phys. **B667**, 170 (2003).
[14] W. E. Caswell, Phys. Rev. Lett. **33**, 244 (1974); T. Banks and A. Zaks, Nucl. Phys. **B196**, 189 (1982).
[15] D. D. Dietrich and F. Sannino, Phys. Rev. D **75**, 085018 (2007).
[16] B. Holdom, Phys. Lett. **150B**, 301 (1985); K. Yamawaki, M. Bando, and K. i. Matumoto, Phys. Rev. Lett. **56**, 1335 (1986); T. W. Appelquist, D. Karabali, and L. C. R. Wijewardhana, Phys. Rev. Lett. **57**, 957 (1986); T. Appelquist and L. C. R. Wijewardhana, Phys. Rev. D **35**, 774 (1987); **36**, 568 (1987); A. G. Cohen and H. Georgi, Nucl. Phys. **B314**, 7 (1989); V. A. Miransky, T. Nonoyama, and K. Yamawaki, Mod. Phys. Lett. A **4**, 1409 (1989); V. A. Miransky and K. Yamawaki, Phys. Rev. D **55**, 5051 (1997); **56**, 3768(E) (1997); T. Appelquist, J. Terning, and L. C. R. Wijewardhana, Phys. Rev. Lett. **77**, 1214 (1996); E. Eichten and K. D. Lane, Phys. Lett. **90B**, 125 (1980); K. D. Lane and E. Eichten, Phys. Lett. B **222**, 274 (1989).
[17] S. Weinberg, Phys. Rev. D **19**, 1277 (1979); L. Susskind, Phys. Rev. D **20**, 2619 (1979).
[18] D. D. Dietrich, F. Sannino, and K. Tuominen, Phys. Rev. D **72**, 055001 (2005).
[19] D. D. Dietrich, F. Sannino, and K. Tuominen, Phys. Rev. D **73**, 037701 (2006).
[20] A. Belyaev, R. Foadi, M. T. Frandsen, M. Jarvinen, F. Sannino, and A. Pukhov, Phys. Rev. D **79**, 035006 (2009).
[21] S. B. Gudnason, C. Kouvaris, and F. Sannino, Phys. Rev. D **73**, 115003 (2006); **74**, 095008 (2006); C. Kouvaris, Phys. Rev. D **76**, 015011 (2007); **78**, 075024 (2008); M. Y. Khlopov and C. Kouvaris, Phys. Rev. D **77**, 065002 (2008); **78**, 065040 (2008); T. A. Ryttov and F. Sannino, Phys. Rev. D **78**, 115010 (2008); K. Belotsky, M. Khlopov, and C. Kouvaris, Phys. Rev. D **79**, 083520 (2009); R. Foadi, M. T. Frandsen, and F. Sannino, Phys. Rev. D **80**, 037702 (2009).
[22] See, for example, D. K. Hong and H. U. Yee, Phys. Rev. D **74**, 015011 (2006); D. D. Dietrich and C. Kouvaris, Phys. Rev. D **78**, 055005 (2008); **79**, 075004 (2009); D. D. Dietrich, M. Jarvinen, and C. Kouvaris, arXiv:0908.4357.
[23] See, for example, T. Appelquist and R. Shrock, Phys. Lett. B **548**, 204 (2002); Phys. Rev. Lett. **90**, 201801 (2003); N. D. Christensen and R. Shrock, Phys. Lett. B **632**, 92 (2006).
[24] M. E. Peskin, Nucl. Phys. **B175**, 197 (1980).
[25] D. D. Dietrich and M. Jarvinen, Phys. Rev. D **79**, 057903 (2009).
[26] O. Antipin and K. Tuominen, arXiv:0912.0674.
[27] O. Antipin and K. Tuominen, Phys. Rev. D **81**, 076011 (2010).
[28] T. Appelquist, K. D. Lane, and U. Mahanta, Phys. Rev.

Lett. **61**, 1553 (1988).
[29] G. Mack, Commun. Math. Phys. **55**, 1 (1977); M. Flato and C. Fronsdal, Lett. Math. Phys. **8**, 159 (1984); V. K. Dobrev and V. B. Petkova, Phys. Lett. **162B**, 127 (1985); N. Seiberg, Nucl. Phys. **B435**, 129 (1995).
[30] F. Sannino, Phys. Rev. D **80**, 065011 (2009); Nucl. Phys. **B830**, 179 (2010).
[31] F. Sannino, Phys. Rev. D **79**, 096007 (2009).
[32] T. A. Ryttov and F. Sannino, arXiv:0906.0307.
[33] A. Armoni, Nucl. Phys. **B826**, 328 (2010); Phys. Rev. D **78**, 065017 (2008).
[34] E. Poppitz and M. Unsal, J. High Energy Phys. 09 (2009) 050; 12 (2009) 011; M. T. Frandsen, T. Pickup, and M. Teper, arXiv:1007.1614.
[35] H. Gies and J. Jaeckel, Eur. Phys. J. C **46**, 433 (2006); J. Braun and H. Gies, Phys. Lett. B **645**, 53 (2007).
[36] F. Sannino and K. Tuominen, Phys. Rev. D **71**, 051901 (2005).
[37] C. Amsler *et al.* (Particle Data Group), Phys. Lett. B **667**, 1 (2008).
[38] A. J. Hietanen, J. Rantaharju, K. Rummukainen, and K. Tuominen, J. High Energy Phys. 05 (2009) 025; S. Catterall and F. Sannino, Phys. Rev. D **76**, 034504 (2007); S. Catterall, J. Giedt, F. Sannino, and J. Schneible, J. High Energy Phys. 11 (2008) 009; arXiv:0910.4387; L. Del Debbio, M. T. Frandsen, H. Panagopoulos, and F. Sannino, J. High Energy Phys. 06 (2008) 007; L. Del Debbio, A. Patella, and C. Pica, Phys. Rev. D **81**, 094503 (2010); Y. Shamir, B. Svetitsky, and T. DeGrand, Phys. Rev. D **78**, 031502 (2008); L. Del Debbio, B. Lucini, A. Patella, C. Pica, and A. Rago, Phys. Rev. D **80**, 074507 (2009); Z. Fodor, K. Holland, J. Kuti, D. Nogradi, and C. Schroeder, Phys. Lett. B **681**, 353 (2009); A. J. Hietanen, K. Rummukainen, and K. Tuominen, Phys. Rev. D **80**, 094504 (2009); F. Bursa, L. Del Debbio, L. Keegan, C. Pica, and T. Pickup, Phys. Rev. D **81**, 014505 (2010).
[39] S. J. Brodsky, G. F. de Teramond, and A. Deur, arXiv:1002.4660; Phys. Rev. D **81**, 096010 (2010).